

Analysis of conjugate mixed convection-conduction heat transfer in a vertical heat generating cylinder immersed in power-law fluids

R. Kouhikamali*, S.M.A. Noori Rahim Abadi, S.M. HosseinNia, S. KhanMohammadi

Department of mechanical engineering, Faculty of engineering, University of Guilan, Rasht, Iran,

*Corresponding author Tel.: +98 131 6690276; E-mail address: kouhikamali@guilan.ac.ir, Fax: +98 131 6690273

ABSTRACT

Conjugate mixed convection-conduction heat transfer from a circular cylinder submerged in power-law fluid has been investigated numerically. The steady two-dimensional conduction equation for the heating cylinder and steady two-dimensional laminar boundary layer equations for the flowing fluid are solved simultaneously using finite difference scheme. The effect of conduction-convection parameter, length to diameter ratio, heat generating, power law viscosity index, Prandtl and Richardson numbers on the temperature distribution in the cylinder and velocity and temperature distributions in the boundary layer are studied. Results showed the axial and radial velocity distributions in the boundary layer and the temperature of the cylinder increase as the heat generating parameter Q , conduction-convection parameter Fi and Richardson number increase. It is also observed that, increasing the Prandtl number decreases the velocity distributions in the boundary layer and on the contrary increases the temperature of the cylinder.

Keywords: Conjugate, Heat Transfer, Vertical Cylinder, Power-Law Fluid

1. Introduction

Conjugate mixed convection heat transfer around a vertical cylinder and conduction heat transfer inside it, is a very interesting subject in heat transfer area. Conjugate heat transfer has a lot of application in different industries. The heat transfer around and inside a fuel bar in the heart of a nuclear reactor in a power plant is one of them. It is clear that the heat transfer from a cylinder goes directly to the ambient fluid. So the fluid characteristic around the cylinder is very important. According to widespread use of the non-Newtonian fluid in different devices, it is vital to investigate their characteristic as the fluid that surrounded the cylinder or a flat plate.

There are lots of researchers who worked on different type of the present study. In other words, some have investigated mixed convection-conduction in Newtonian liquids; some have studied the forced convection in a cylinder with or without heat generation. There are several combinations of laminar, mixed or forced convection heat transfer with considering the conduction inside the cylinder meanwhile the heat generation in the cylinder can be involved. In addition, another important matter of discussion in this area is simulating the conjugate mixed convection-conduction heat transfer in porous media.

The conjugate mixed convection-conduction heat transfer along a vertical cylindrical fin in non-Newtonian fluids has been studied by Wang [1]. He used the appropriate variable transformations to reduce the original partial differential equations to the non-similar equations with a coupling of the energy equation of fin through the interfacial conditions. An implicit finite difference is employed to solve the equations of fluid and the Gaussian elimination method is used to deal the energy equation of fin. Wang [1] did not consider the heat generation in the cylinder.

Jilani [2] et al. worked on the radial heat conduction along with heat generation in a vertical cylinder. They solved the

steady two-dimensional conduction equation for cylinder and steady two-dimensional forced laminar boundary layer equations for the flowing fluid simultaneously with a finite difference scheme. As mentioned, one important application of conjugate heat transfer theory is in nuclear reactors. This problem was studied by Ramis et al. [3]. A comparative study of uniform and non-uniform volumetric heat generation in a rectangular nuclear fuel element was investigated numerically. This fuel element was washed by liquid sodium. The boundary layer equations governing the flow and thermal fields in the fluid domain are solved numerically along with two-dimensional heat conduction equation in the solid domain by satisfying the conditions of continuity of temperature and heat flux at the solid-fluid interface

Kumari and Nath [4] investigated a conjugate mixed convection transport from a moving vertical plate in a non-Newtonian fluid. They considered the partial differential equations governing the natural convection flow over a vertical moving surface. They used an implicit finite-difference method to solve the mentioned equations numerically.

K Khellaf, G Lauriat [5] investigated the heat transfer in a non-Newtonian Carreau-fluid between rotating concentric vertical cylinders. Their results show that the shear thinning effect decreases the friction factor at the rotating cylinder and increases the heat transfer through the annular gap. It is also shown that the reduction in apparent viscosity may produce oscillatory flows, especially for centrifugally forced convection. Salman and Mulligan [6] studied the transient free convection from a vertical plate to a non-newtonian fluid in a porous medium. They found that non-Newtonian fluids which are pseudoplastic exhibit a significantly larger change in the heat transfer coefficient during the transition between the initial diffusive and final steady flow conditions, and unlike the free convection in homogeneous media neither dilatants nor pseudoplastics exhibit any undershoot in the heat transfer coefficient. Furthermore, they showed that the time required to reach steady state increases and the heat transfer

coefficient decreases with a decrease in the power law index. Sasmal and Chhabra [7] worked on laminar natural convection from a heated square cylinder immersed in power-law liquids. They have solved the governing equation over wide range of dimensionless parameter such as Grashof number, Prandtl number and power-law index. In their literature it is reported that the obtained results for Newtonian fluid behavior are in excellent agreement with the available experimental data. Chandra and Chhabra [8] extended the previous study as a laminar free convection from a horizontal semi-circular cylinder to power-law fluids. Mamun [9] et al. worked on the heat generation effect on laminar natural convection flow along and conduction inside a vertical flat plate. They used an implicit finite difference method to solve the non-dimensional equations of non-linear equations by introducing a non-similarity transformation. The velocity profiles as well as temperature distributions were studied.

As it was remarked earlier an important part on conjugate mixed convection conduction where is widely investigated is in porous media. Liu et al. [10] has investigated the problem of conjugate mixed convection-conduction heat transfer along a cylindrical fin in a porous medium analytically. They used a local non similarity solution for the convective flow in the porous medium. As it is reported in their paper the trends of the results obtained, are similar to those of plate fin solution. It means if the radii of curvature set to be infinite, the results are the same as a flat plate. Liu et al. [11] studied the conjugate natural convection about a vertical cylinder with lateral mass flux in a saturated porous medium. They have attempted the influence of injection or withdrawal of fluids on the conjugate heat transfer. The effect of surface mass flux, the conjugate convection-conduction parameter and the surface curvature on fin temperature distribution, local heat transfer coefficient, local heat flux, average heat transfer coefficient and total heat transfer rate are presented in their work. The obtained results have been compared with finite-difference solutions for the case of constant wall temperature and a good agreement is achieved. The problem of unsteady free convection with heat and mass transfer from an isothermal vertical flat plate on a non-Newtonian power law saturated porous medium has studied by Elgazery [12]. The finite difference method was used to carry out the various parameters entering into the problem such as velocity, temperature and concentration profiles.

Kim et al. [13] studied the influence of internal shape of open 'cavities' exerts on the Constructal design of a heat generating body. Several shapes of cavity were studied; triangular, elliptical, trapezoidal and Y-shaped cavities intruding into a trapezoidal shaped solid with uniform heat generation. They tried to is minimize the peak (hot spot) temperature with respect to the geometrical parameters of the system. They found that, utilizing the triangular and Y- Shaped cavities can result more reliable and effective rather than other studied cavities. Lorenzini and Biserni [14] investigated the thermal and fluid-dynamic behaviour of laminar mixed convection in a non-Newtonian fluid inside a vertical duct enclosed within two vertical plates that are plane and parallel, having linearly varying wall temperatures, numerically. Their quantitative results of the analysis, which were strongly affected by the variation of the Grashof number and of the exponent of the power law, were given in terms of graphic visualisations of the fluid velocity profiles and, when the governing parameters vary, of the various geometries characterising the heat transfer. Lorenzini et al. [15] studied the geometrical optimization of a complex cavity, namely a T-Y-shaped

cavity with two additional lateral intrusions into a solid conducting wall. The objective was to minimize the global thermal resistance between the solid and the complex assembly of cavities. Their analysis demonstrated that not all degrees of freedom play the same role in the performance of the complex cavity design. Also an improvement of approximately 45% has been observed after the optimization of the ratio H_3/L_3 while the optimization of the parameters H_1/L_1 and H_2/L_2 led to an additional gain of only 1%.

In the present work conjugate mixed convection-conduction heat transfer from a circular cylinder submerged in power-law fluid has been investigated numerically. The effect of conduction-convection parameter, length to diameter ratio, heat generating, power law viscosity index, Prandtl and Richardson numbers on the temperature distribution in the cylinder and velocity and temperature distributions in the boundary layer are studied.

2. Problem statement and mathematical formulation

Many different types of non-Newtonian fluids exist but the simplest and most common type is the power-law fluid for which the theological equation of state between stress components and strain rate components defined by Vujanovic et al. [16]:

$$\tau_{i,j} = -P\delta_{i,j} + K \left| \sum_{m=1}^3 \sum_{l=1}^3 e_{lm} e_{lm} \right|^{(n-1)/2} e_{i,j} \quad (1)$$

Where P is the pressure, $\delta_{i,j}$ is the Kronecker delta and K and n are the consistency and flow behavior indices of the fluid. When $n > 1$ the fluid is described as dilatant, $n < 1$ as pseudo-plastic and when $n = 1$ it is known as the Newtonian fluid.

Consider the steady, laminar boundary layer in a two-dimensional mixed convective flow of a non-Newtonian fluid along a vertical heat-generating circular cylinder. The lower end of the cylinder is assumed to be maintained at T_b while the upper end is insulated, as shown in Fig. 1.

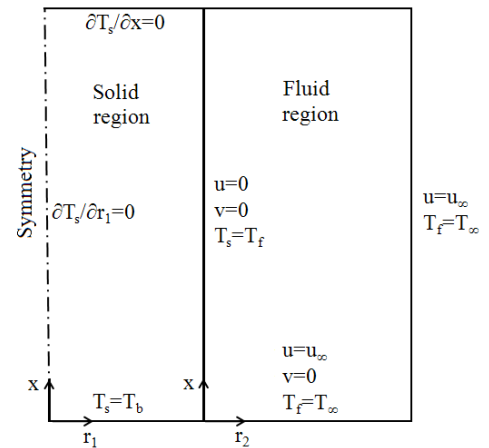


Figure 1. Physical problem

In the case that upper end of cylinder is insulated, the heat transfer mechanism can be divided in two mechanisms: (1) Conduction heat transfer inside the cylinder and (2) Convection heat transfer from the cylinder surface to the fluid. The temperature distribution inside the cylinder is governed by two dimensional conduction heat transfer equation while the temperature and velocity profile in the flow fluid are governed by the boundary layer equations.

In order to carry out a precise analysis a set of assumptions are made as follow:

- (a) The variation of thermo-physical properties of the fluid is neglected.
- (b) The flow is incompressible, steady, laminar and two dimensional.
- (c) The thermal conductivity of the cylinder does not change with temperature.
- (d) The heat generation is uniform in cylinder.

Symmetrical geometry of cylinder about centerline and fluid flow enables to solve only half of the computational domain to obtain two dimensional temperature distributions inside the cylinder.

Under these assumptions with the usual Boussinesq approximation, the governing boundary-layer equations that are based on the balance laws of mass, linear momentum and energy for the fluid flow region can be written as:

$$\frac{\partial u}{\partial x} + \frac{1}{r_2} \frac{\partial}{\partial r_2} (r_2 v) = 0 \quad (2)$$

$$u \frac{\partial u}{\partial x} + v \frac{\partial u}{\partial r_2} = g \beta (T_f - T_\infty) + \frac{K}{\rho r_2} \left[\frac{\partial}{\partial r_2} \left(r_2 \left| \frac{\partial u}{\partial r_2} \right|^{n-1} \right) \frac{\partial u}{\partial r_2} \right] \quad (3)$$

$$u \frac{\partial T_f}{\partial x} + v \frac{\partial T_f}{\partial r_2} = \frac{\alpha}{r_2} \frac{\partial}{\partial r_2} \left(r_2 \frac{\partial T_f}{\partial r_2} \right) \quad (4)$$

The two dimensional form of energy equation in solid region (cylinder) can be written as follow:

$$\frac{\partial^2 T_s}{\partial x^2} + \frac{\partial^2 T_s}{\partial r_1^2} + \frac{1}{r_1} \frac{\partial T_s}{\partial r_1} + Q = 0 \quad (5)$$

The boundary conditions for solving these equations will be as follows:

$$u(0, r_2) = u_\infty, \quad v(0, r_2) = 0, \quad T_f(x, 0) = T_s(x, D)$$

$$T_f(x, \infty) = T_\infty, \quad u(x, \infty) = u_\infty$$

$$T_s(0, r_1) = T_b$$

$$\left. \frac{\partial T_s}{\partial r_1} \right|_{r_1=0} = 0, \quad \left. \frac{\partial v}{\partial r_2} \right|_{r_2=0} = 0$$

$$\begin{cases} T_f(0, r_2) = T_\infty & r_2 > 0 \\ T_f(0, r_2) = T_s & r_2 = 0 \end{cases}$$

and at the interface:

$$k_s \frac{\partial T_s}{\partial r_1}(x, D) = k_f \frac{\partial T_f}{\partial r_2}(x, 0) \quad (6)$$

In order to obtain dimensional form of above equations some dimensionless variable is used. The dimensionless variables can be defined as follow:

$$\begin{aligned} x^* &= \frac{x}{L} \\ r_1^* &= \frac{r_1}{r_0}, \quad r_2^* = \frac{r_2}{L} \\ u^* &= \frac{u}{U_\infty}, \quad v^* = \frac{v}{U_\infty} \\ \theta &= \frac{T - T_\infty}{T_b - T_\infty}, \quad Q^* = \frac{QD^2}{4k_s(T_b - T_\infty)} \\ \text{Re} &= U_\infty \frac{L}{\nu}, \quad \text{Pr} = \frac{\nu}{\alpha}, \quad \text{Gr} = \frac{g\beta L^3 \Delta \theta}{\nu^2} \\ D &= 2r_0, \quad \text{Fi} = \frac{k_s}{k_f}, \quad Z = \frac{D}{2L}, \quad U_\infty = \left[\frac{\rho L^n}{k} \right]^{\frac{1}{n-2}} \end{aligned} \quad (7)$$

By using the aforementioned dimensionless variables the continuity, momentum and energy equation can be written as follow. It should be mentioned the star is omitted for simplicity in the following formula:

Continuity:

$$\frac{\partial u}{\partial x} + \frac{1}{r_2} \frac{\partial}{\partial r_2} (r_2 v) = 0 \quad (8)$$

Momentum:

$$u \frac{\partial u}{\partial x} + v \frac{\partial u}{\partial r_2} = \frac{\text{Gr}}{\text{Re}^2} \theta_f + \frac{1}{r_2} \left[\frac{\partial}{\partial r_2} \left(r_2 \left| \frac{\partial u}{\partial r_2} \right|^{n-1} \right) \frac{\partial u}{\partial r_2} \right] \quad (9)$$

Energy in fluid field:

$$u \frac{\partial \theta_f}{\partial x} + v \frac{\partial \theta_f}{\partial r_2} = \frac{1}{\text{Re Pr}} \frac{\partial}{\partial r_2} \left(r_2 \frac{\partial \theta_f}{\partial r_2} \right) \quad (10)$$

Energy in solid field:

$$Z^2 \frac{\partial^2 \theta_s}{\partial x^2} + \frac{\partial^2 \theta_s}{\partial r_1^2} + \frac{1}{r_1} \frac{\partial \theta_s}{\partial r_1} + Q = 0 \quad (11)$$

The boundary conditions in dimensionless form can be presented as follow:

$$\begin{aligned} u(0, r_2) &= 1 & u(x, 0) &= 0 & u(x, \infty) &= 1 \\ v(0, r_2) &= 0 & v(x, 0) &= 0 & \frac{\partial v}{\partial r_2}(x, \infty) &= 0 \\ \theta_f(0, r_2) &= 0 & \theta_f(x, \infty) &= 0 & \theta_f(x, 0) &= \theta_s(x, 1) \\ \theta_s(0, r_1) &= 1 & \frac{\partial \theta_s}{\partial r_1}(x, 0) &= 0 & \text{Z.Fi} \frac{\partial \theta_s}{\partial r_1}(x, 1) &= \frac{\partial \theta_f}{\partial r_2}(x, 0) \end{aligned} \quad (12)$$

3. Numerical method and computational procedure

Governing equations show the problem is a conjugate heat transfer (Eqs. (8)-(11)). Caused by the presence of nonlinear term in momentum boundary layer equation and coupling energy and momentum equations, it is inventible using a finite difference method. The steady non-linear coupled equations (Eqs. (8)-(11)) subject to the boundary conditions (12) are solved by using an implicit finite-difference scheme. The solution begins with solving boundary layer equations (Eqs. (8)-(10)) with a supposed temperature distribution along cylinder. In the next step, Eq. (11) with conjugate boundary condition is solved using updated temperature distribution in the flow field. The improved surface temperature distribution is again used in solving boundary layer equations. The loop is repeated until a reasonable convergence of cylinder surface temperature is obtained. The boundary layer equations are parabolic in x-direction and can be solved by marching procedure. The two dimensional conduction heat transfer equation is elliptic type and is solved using line by line method.

4. Results and discussion

4.1. Validation and grid dependency

To obtain an optimal computational grid for this study, a grid independency test is performed for a particular case as shown in Fig. 2. Three types of grids were considered for the grid independency inspection. The coarse grid and moderate grid is made of 51*51*51 and 101*101*101 computational cells respectively and the fine mesh is made of 201*201*201

computational cells. Based upon the mesh sensitivity results, a non-uniform structured computational grid with 201*201*201 nodes was used for all other cases in r_1 , x , r_2 direction, respectively.

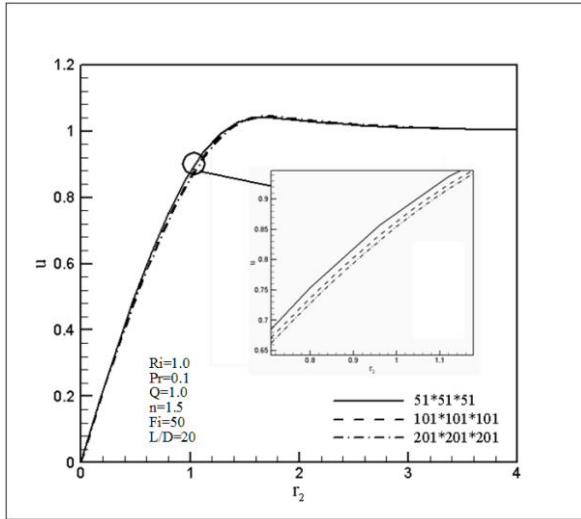


Figure 2. Variations of axial velocity for different grid sizes at $x=0.1$.

The local Nusselt number is calculated as follows:

$$Nu_l = \frac{-\frac{\partial \theta_f}{\partial r_2} \big|_{r_2=r_0}}{\theta_s \big|_{r_1=r_0}} \quad (13)$$

And the average Nusselt number along the surface of the cylinder is illustrated as follow:

$$Nu_{ave} = \int_0^L Nu_l dx \quad (14)$$

Table 1 compares the present values of average Nusselt number with that of the values of Acrivos [17] and the numerical results of Avinash Chandra and R.P. Chhabra [8]. The results show good agreement with their results.

Table 1. Comparison of the present values of the average Nusselt number with literature values.

n	$Gr^{(1/(2n+1))} Pr^{(n/(3n+1))}$	Avinash Chandra and R.P. Chhabra [8]	Acrivos [17]	Present work
1.0	1.638	1.872	1.376	1.77
1.5	1.449	1.670	1.304	1.65
1.8	1.375	1.622	-	1.64

4.2. Velocity and temperature profiles

The dimensionless axial velocity in x direction " u " at various x -locations on the cylinder is shown in Fig. 3. The profile near the leading edge has steeper gradient compared to that away from it. This trend shows the growth of boundary layer in the axial direction. The non-similar nature of the flow is evident from the dependence of these profiles on the value of x .

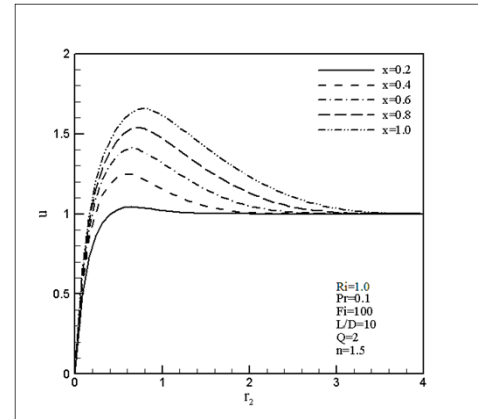


Figure 3. Longitudinal velocity distribution in the boundary layer at different x -locations.

Fig. 4 illustrates the dimensionless radial velocity profiles at different axial locations. It is obvious that the radial velocity up to some distance from the leading edge, increases at first and then decreases. This is due to the fact that entrainment of the fluid into the boundary layer is more near the leading edge compared to that from it. These profiles also show the non-similar nature of the flow.

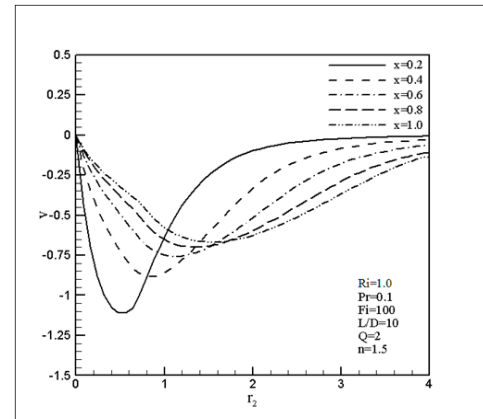


Figure 4. Transverse velocity distribution in the boundary layer at different x -locations.

Fig. 5 shows the radial temperature distribution in the boundary layer at various axial locations. Development of the thermal boundary layer is faster than that of velocity boundary layer.

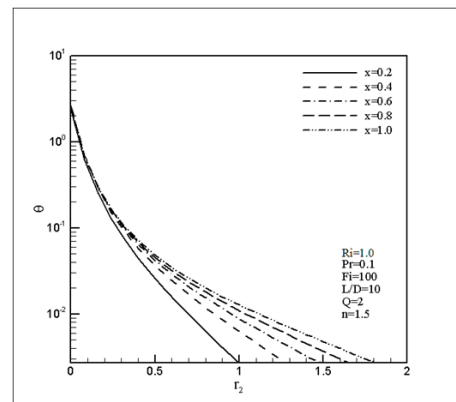


Figure 5. Temperature distribution in the boundary layer at different x -locations.

It is also observed the radial temperature distribution becomes steeper along the axial direction. It is due to the fact that the flux from the surface of the cylinder near the leading edge is more than that away from it. However, increase in temperature is rapidly reduced after $x=0.6$. This trend reveals important fact as the-temperature in the cylinder must be kept below certain allowable limit.

Fig. 6. Effect of L/D ratio on (a) temperature distribution in the cylinder (b) temperature distribution in the boundary layer (c) longitudinal velocity distribution in the boundary layer (d) transverse velocity in the boundary layer at $x=0.1$.

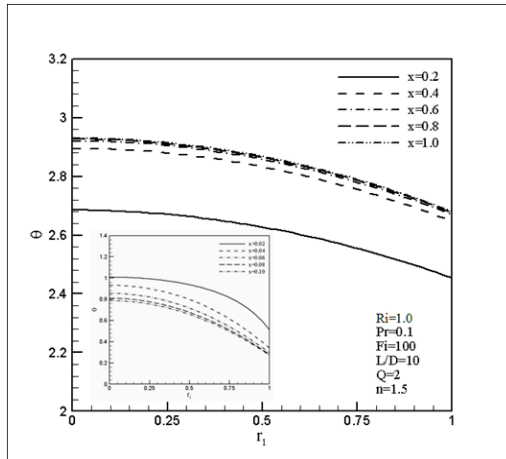


Figure 6. Temperature distribution in the cylinder at different x -locations.

4.3. Effect of conduction-convection parameter

The effect of conduction-convection parameter on temperature distribution at the boundary layer is illustrated in Fig. 7 (a). As Fi increases, the thickness of the thermal boundary layer increases. This is due the fact that increase in Fi is mainly due to the thermal conductivity of the flowing fluid. Decrease in Fi , results in higher dissipation to the fluid which is most desirable in many industrial applications. Moreover, decrease in Fi results in lower temperature distribution in cylinder (Fig. 7 (b)). The maximum temperature at the center of the cylinder has similar trend. This is due to the fact that energy dissipation to the flowing flow increases as the value of Fi decreases.

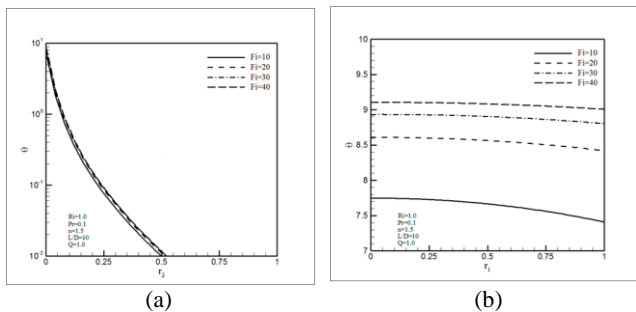


Figure 7. Effect of conduction-convection parameter on temperature distribution (a) in the boundary layer (b) in the cylinder at $x=0.1$.

4.4. Effect of heat generation parameter

Figs. 8 (a) and (b) show the distribution of temperature profiles of the fluid and the cylinder, respectively. It is clear that increase in Q increases the thickness of the boundary

layer. Even though there is significant change in the temperature gradient in the boundary layer, the temperature of the fluid is increased overall. It is also observed that increase in Q will result in increase in the surface temperature of the cylinder. Based on the above observation it should be noticed there is a limit for Q to increase.

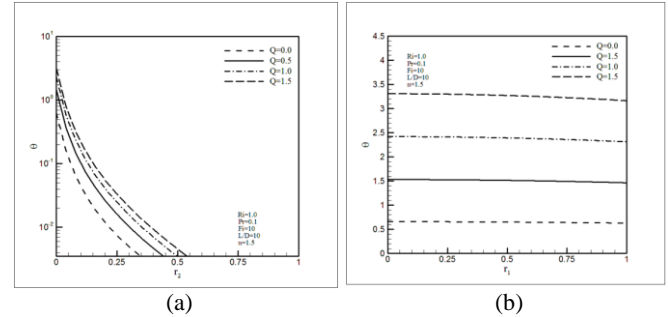


Figure 8. Effect of heat generating parameter on temperature distribution (a) in the boundary layer (b) in the cylinder at $x=0.1$.

4.5. Effect of power law viscosity index

Figs. 9 (a) and (b) show the axial and radial velocity profiles for different values of flow index parameter n . It is clear as n increases the axial velocity decreases. It is due the fact that the momentum boundary layer thickness increases as n increases. It is also shown the radial velocity tends to lower values as the value of n increases.

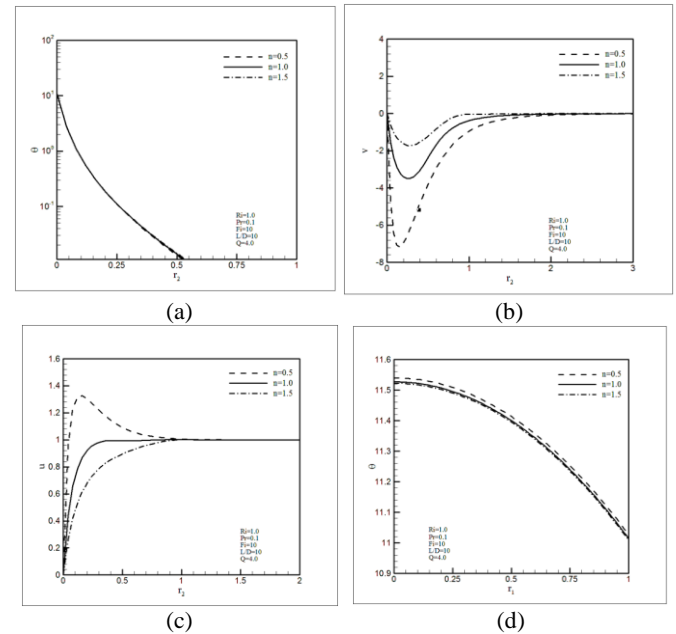


Figure 9. Effect of power law viscosity index on (a) longitudinal velocity distribution in the boundary (b) transverse velocity distribution in the boundary (c) temperature distribution in the boundary layer (d) temperature distribution in the cylinder at $x=0.1$.

The temperature distributions in the boundary layer and the cylinder are shown in Figs. 9 (c) and (d), respectively. It is evident that the temperature profiles do not change significantly with increase in n . It is due to the fact that thermal boundary layer thickness remains almost unchanged.

4.6. Effect of L/D ratio

Figs. 10 (a) and (b) show the effect of length to diameter on temperature distributions of the cylinder and the boundary layer, respectively. The higher value of L/D ratio corresponds to higher flow Reynolds number which gives rise to higher convective heat transfer coefficient resulting in higher rate of energy dissipation to the fluid. However, all dissipated energy to the fluid in radial direction may not be carried away by the flowing flow. This may be the reason that is slight increase in temperature of the fluid. As mentioned above increase in L/D ratio results in increase in higher Reynolds number which corresponds to lower effect of natural convection. Therefore, as it is seen in Fig. 10 (c) the peak of axial velocity profile decreases with increasing the ratio L/D. Also the radial profile tends to the lower values due to the fact that the force convection becomes dominated (Fig. 10 (d)).

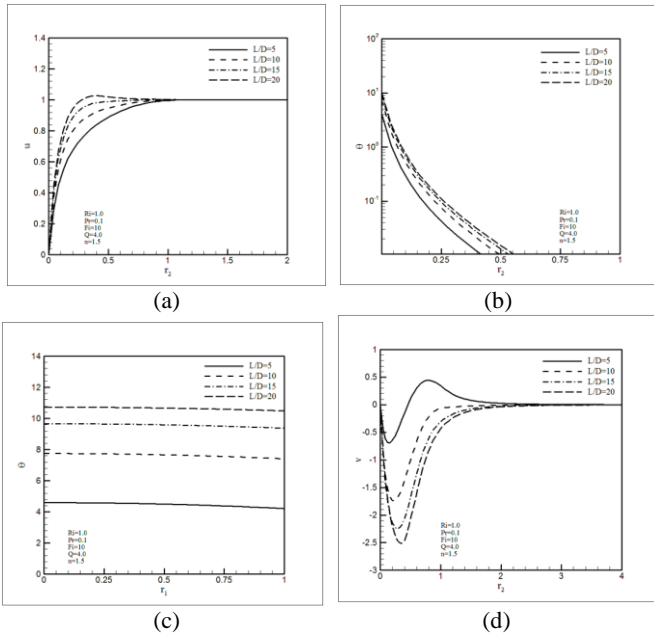


Figure 10. Effect of L/D ratio on (a) temperature distribution in the cylinder (b) temperature distribution in the boundary layer (c) longitudinal velocity distribution in the boundary layer (d) transverse velocity in the boundary layer at $x=0.1$.

4.7. Effect of Richardson number

Figs. 11 (a) and (b) show the effect of buoyancy parameter Ri on the axial and radial velocity distributions. As it can be seen from Fig. 11 (a), the axial velocity increases with increase in Ri number. The physical reason is that the assisting buoyancy force implies favorable pressure gradient and the fluid gets accelerated which results in thinner momentum and thermal boundary layers. Due to natural dominated regime at higher Ri number the radial velocities tends to more negative values. It is also observed that heat flux increases with increasing Ri number due to increased buoyancy effects, as a result the temperature distribution in cylinder will increase (Fig. 11 (c)).

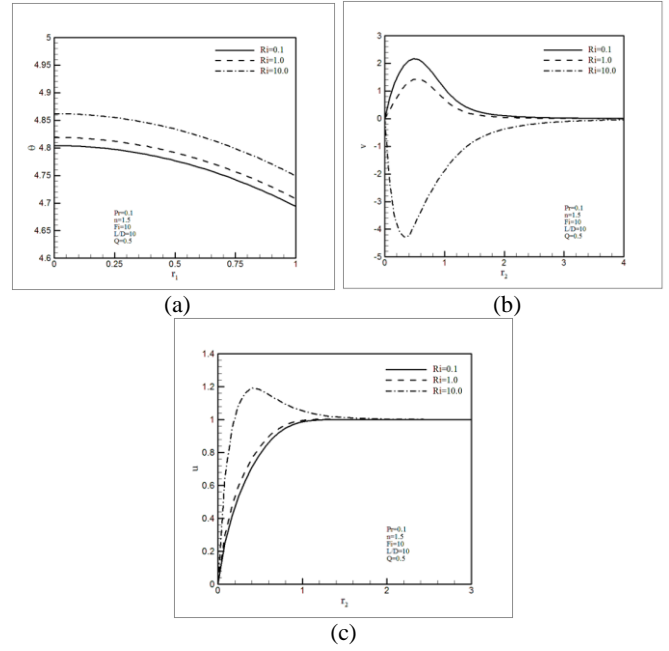


Figure 11. Effect of Ri number on (a) longitudinal velocity distribution in the boundary (b) transverse velocity in the boundary layer (c) longitudinal temperature distribution in the cylinder at $x=0.1$.

4.8. Effect of Prandtl number

The velocity boundary layer thickness decreases with increasing values of Prandtl number. Therefore as shown in Figs. 12 (a) and (b), increasing in the values of Pr, causes the axial and radial velocities to decrease significantly. Figs. 12 (c) and (d) illustrate the temperature distributions in the boundary layer and the cylinder, respectively. The thermal boundary thickness of boundary layer decreases which results in increase in cylinder and fluid temperatures.

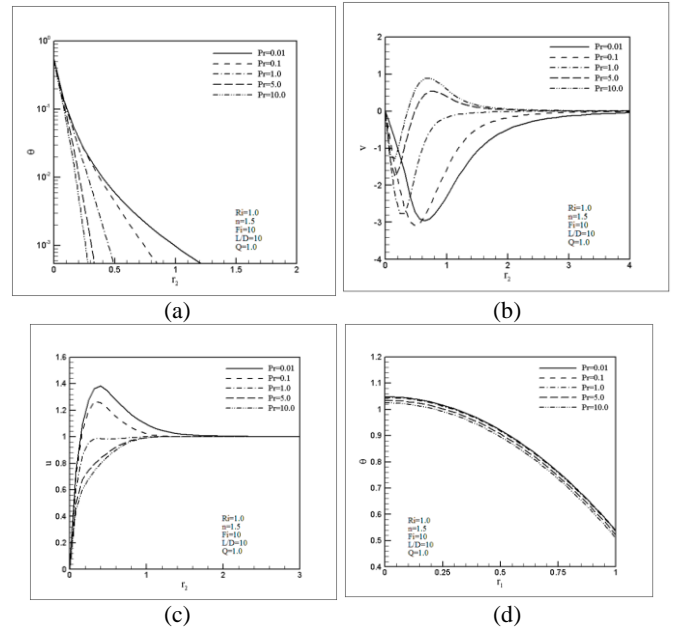


Figure 12. Effect of Pr number on (a) longitudinal velocity distribution in the boundary (b) transverse velocity distribution in the boundary (c) temperature distribution in the boundary layer (d) temperature distribution in the cylinder at $x=0.1$.

Also the higher Prandtl number fluid has a lower thermal conductivity (or a higher viscosity) which results in thinner thermal boundary layer and hence, higher heat transfer rate at the surface.

5. Conclusion

In this article mixed convection heat transfer from a circular cylinder submerged in power-law fluid had been studied numerically. The effect of conduction-convection parameter, length to diameter ratio, heat generating, flow index for power-law fluid, Prandtl and Richardson numbers on the temperature distribution in the cylinder and velocity and temperature distributions in the boundary layer were investigated. The results showed the axial and radial velocity distributions in the boundary layer and the temperature of the cylinder increase as the heat generating parameter Q , conduction-convection parameter Fi and Richardson number increase. It is also observed increase in Prandtl number decreases the velocity distributions in the boundary layer and on the contrary increases the temperature in the cylinder.

Nomenclature:

Fi	conduction-convection parameter
K	flow consistency index for power-law fluid
k_s	thermal conductivity of cylinder
k_f	thermal conductivity of fluid
L	characteristic length of the cylinder
n	power law viscosity index
Z	parameter representing length to diameter ratio of the cylinder
Pr	Prandtl number
Q	internal heat generating per unit volume in the cylinder
r_1	radial coordinate used in two-dimensional heat conduction equation
r_2	radial coordinate normal to the cylinder surface
Re	Reynolds number
Gr	Grashof number
Ri	Richardson number
Nu_l	local Nusselt number
Nu_{ave}	average Nusselt number
T	temperature
u	velocity component in x-direction
v	velocity component in r-direction
x	stream-wise coordinate along the cylinder length
g	gravitational acceleration
f	fluid
s	solid

Greek symbols

θ	non-dimensional temperature
β	fluid thermal expansion coefficient
ρ	fluid density
α	thermal diffusivity
∞	free stream

References:

1. Tian-Yih Wang, Conjugate mixed convection-conduction heat transfer along a vertical fin in non-Newtonian fluids, *Int. Commun. Heat Mass Transfer* 21 (1994) 583-596.
2. G. Jilani, S. Jayaraj, M. Adeel Ahmad, Conjugate forced convection-conduction heat transfer analysis

- of a heat generating vertical cylinder, *Int. J. Heat Mass Transfer* 45 (2002) 331-341.
3. M.K. Ramis, G. Jilani, S. Jahangeer, Conjugate conduction-forced convection heat transfer analysis of a rectangular nuclear fuel element with non-uniform volumetric energy generation, *Int. J. Heat Mass Transfer* 51 (2008) 517-525.
4. Mahesh Kumari, Girishwar Nath, Conjugate mixed convection transport from a moving vertical plate in a non-Newtonian fluid, *Int. J. Therm. Sci.* 45 (2006) 607-614.
5. K Khellaf, G Lauriat, Numerical study of heat transfer in a non-Newtonian Carreau-fluid between rotating concentric vertical cylinders. *J. Non-Newtonian Fluid Mech.* 89 (2000) 45-61.
6. Salman Haq, J.C. Mulligan, Transient free convection from a vertical plate to a non-newtonian fluid in a porous medium *J. Non-Newtonian. Fluid Mech.* 36 (1990) 395-410.
7. C. Sasmal, R.P. Chhabra, Laminar natural convection from a heated square cylinder immersed in power-law liquids, *J. Non-Newtonian Fluid Mech.* 166 (2011) 811-830.
8. Avinash Chandra, R.P. Chhabra, Laminar free convection from a horizontal semi-circular cylinder to power-law fluids, *Int. J. Heat Mass Transfer* 55 (2012) 2934-2944.
9. A.A. Mamun, Z.R. Chowdhury, M.A. Azim, M.A. Maleque, Conjugate heat transfer for a vertical flat plate with heat generation effect, *Nonlinear Anal. Modell. Control.* 13 (2008) 213-223.
10. Jin Yuan Liu, W. J. Minkowycz, P. Cheng, Conjugate mixed convection-conduction heat transfer along a cylindrical fin in a porous medium, *Int. J. Heat Mass Transfer* 29 (1986) 769-775.
11. Jin-Yuan Liu, Shagi-Di Shih, W.J. Minkowycz, Conjugate natural convection about a vertical cylindrical fin with lateral mass flux in a saturated porous medium, *Int. J. Heat Mass Transfer* 30 (1987) 623-630.
12. Nasser S. Elgazery, Transient analysis of heat and mass transfer by natural convection in power-law fluid past a vertical plate immersed in a porous medium, *J. Appl. Appl. Math.* 3 (2008) 267-285.
13. Y. Kim, S. Lorente and A. Bejan, Steam Generator Structure: Continuous Model and Constructal Design, *Int. J. Energy Res.* 35 (2011) 336-345.
14. G. Lorenzini, C. Biserni, Numerical investigation on mixed convection in a non-newtonian fluid inside a vertical duct, *Int. J. Therm. Sci.*, 43 (2004) 1153-1160.
15. G. Lorenzini, F.L. Garcia, E.D. Dos Santos, C. Biserni, L.A.O. Rocha, Constructal design applied to the optimization of complex geometries: T-Y-shaped cavities with two additional lateral intrusions cooled by convection, *Int. J. Heat Mass Transf.*, 55 (2012) 1505-1512.
16. B. Vujanovic, A.M. Stauss, Dj. Djukic, A variational solution of the Rayleigh problem for a power law non-Newtonian conducting fluid, *Ing. Arch.* 41 (1972) 381-386.
17. A. Acrivos, A theoretical analysis of laminar natural convection heat transfer to non-Newtonian fluids, *AIChE J.* 6 (1960) 584-590.

